

## A new imaging science test object for performance measurements of ultrasonic imaging systems

Dan Phillips and Kevin J Parker

Rochester Center for Biomedical Ultrasound, Department of Electrical Engineering, University of Rochester, Rochester, NY 14627, USA

Received 2 December 1996, in final form 1 August 1997

**Abstract.** We propose a novel test object for ultrasound imaging. The test object, or phantom, is manufactured using thin film techniques allowing precise placement of 'digital scatterers' which can produce sophisticated test targets, similar to those that are widely used in imaging science to evaluate displays, printers and electronic imaging systems. These test objects can be used in conjunction with standard performance evaluation methods and devices to augment and enhance their capabilities and range of application.

### 1. Introduction

The image displayed by an ultrasound scanner is the result of many complex stages and operations. Extensive signal processing is involved in both the transmitted and received signals. When such sophisticated systems form the basis for medical diagnosis and treatment, techniques for comprehensive yet manageable performance evaluation are essential.

There are generally two components necessary for an effective performance evaluation procedure: (i) standard test objects and (ii) methods to evaluate how well the system under consideration measures or images the test objects.

In medical ultrasonic imaging, test objects have typically consisted of an assemblage of target items embedded in some type of material with varying acoustic propagating properties (AIUM 1991). Methods to assess system performance have included characterization of spatial resolution and accuracy as well as discrimination of varying acoustic properties. Various phantoms have produced 'lesions' of different size and echogenicity for lesion detection study (AIUM 1991, ATS Laboratories 1993, Cone Instruments 1993, Madsen *et al* 1978, 1980, Sommer *et al* 1980, Yao *et al* 1991, Alasaarela and Koivukangas 1990, Spitzer *et al* 1979, Smith 1982, Goldstein and Clayman 1983). Other random scatterer regions have been used to assess the beamwidth of an ultrasound transducer (Ophir *et al* 1983). As in imaging science, line and point targets can be added to a background to make basic measurements of distortion and point spread functions (Rose and Weimer 1989, Dainty and Shaw 1974, Carlson 1977).

It has long been recognized (Hill and Kratochwil 1981, Goldstein and Clayman 1983) that methods from the discipline of imaging science should provide valuable information regarding the overall performance of an ultrasound imaging system. Evidence for the continued need for this type of approach is given in the award-winning paper by Hill *et al* entitled 'What might echography learn from image science' (Hill *et al* 1991).

Standard imaging science measurements can be difficult to obtain with conventional ultrasound test objects such as cones, spheres and wires of varying echogenicity. We demonstrate a new class of ultrasound imaging test objects that can be manufactured with precise control of the echogenicity of the target patterns. The requirements for constructing such targets for ultrasound imaging include precise distribution of scatterers on a surface of one or more thin film substrates with control over the local concentration and distribution of the scatterers. This approach is described in the next section.

## 2. A thin film test object with digital scatterers

### 2.1. Thin film propagation

The test object is constructed with a flat substrate supporting a spatial test pattern of ‘digital scatterers’ produced by an appropriate thin film deposition technique. The thin film test object is then oriented coplanar to the scanning plane of the ultrasonic imaging system being evaluated. Assuming that the substrate thickness is much less than a wavelength of the ultrasound pulse, the pulse will propagate at close to the speed of sound of the host medium (Archer-Hall and Hutchins 1979, 1981), and the acoustic inhomogeneities presented by the deposited pattern will produce reflected waves that will be detected and processed by the ultrasound scanner (see figure 1(a)).

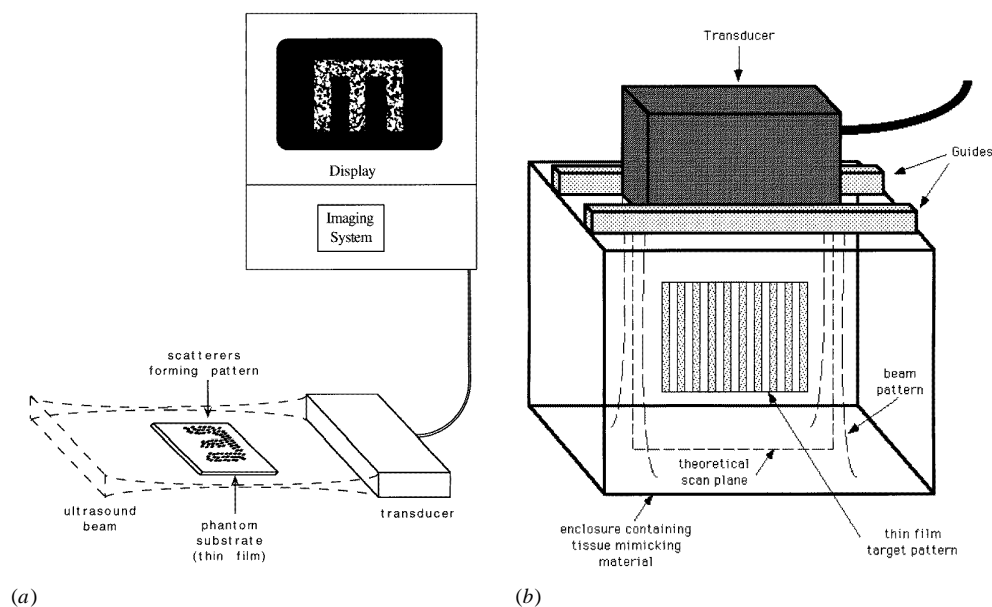


**Figure 1.** (a) Schematic diagram of the concept of a thin film test object. (b) Representation of a simple implementation of a phantom incorporating a thin film test object.

In essence, this technique allows a very controlled volume distribution of scatterers, albeit in a volume of minimal thickness. In this manner, the volume distribution of the scatterers is tightly controlled in two ways: in the 2D scanning plane, the scatterer dimensions are specified by the resolution of the deposited pattern; in the out-of-plane direction of the interrogating beam, the scatterer dimension is determined by the thickness of the deposited pattern.

## 2.2. Scattering

Acoustic scattering results from spatial variations in the acoustic impedance of the insonated material (Morse and Uno 1986). The three acoustic impedances of interest in this case are those of the propagating medium, the test object substrate and the material deposited on the substrate that forms the thin film pattern used for evaluation. Since this test object is to be used for evaluation of medical ultrasound scanners, the propagating medium is normally assumed to have an acoustic impedance close to that of tissue and an attenuation of  $0.3$  to  $1.0 \text{ dB cm}^{-1} \text{ MHz}^{-1}$  as suggested by the AIUM guidelines (AIUM 1991). The substrate material's acoustic properties need not exactly match those of the propagating medium as long as the material has smooth surfaces and has a thickness on the order of, or less than, the ultrasound wavelength. Finally, the material comprising the deposited scatterers must have an acoustic impedance that is detectably different from that of the propagating medium. As shown in figure 1(a), the scatterers are deposited as a thin film on a substrate which lies coplanar to the plane of the interrogating ultrasound beam (i.e. the test object lies in the plane defined by the azimuthal and range axis relative to the ultrasound transducer). The thin film/substrate assembly is embedded in a tissue equivalent material contained in a fixture that provides coplanar alignment of the beam produced by the transducer under evaluation with the thin film target as shown in figure 1(b).

## 2.3. Precise deposition of 'digital' scatterers

Since we are interested in precise control of the scattering pattern produced in the 2D scanning plane, concentration, size and spacing of the scattering material in the thickness dimension should be predetermined and reproducibly manufactured. The number of scatterers per unit volume is specified and precisely controlled so that a defined regional scattering strength can be produced. The deposited pattern is considered to be 'digital', or 'binary' in nature, since a discrete scatterer is either present or absent at every addressable point on the surface of the thin film. The plane of the substrate consists of areas, at a given resolution, that either scatter with specified characteristics or will not scatter at all. This permits the use of established half-tone techniques for the purposes of providing the scattering analogue of the visual gray scale.

In the foregoing discussion, it is assumed that the ability to specify the number and location of 'digital scatterers' is on a scale much finer than that of a wavelength produced by the ultrasound imaging system being evaluated. For a diagnostic scanner with a 5 MHz transducer in soft tissue, one wavelength corresponds to approximately  $300 \mu\text{m}$ . Even a common 300 dpi (dots per inch) laser printer using  $10 \mu\text{m}$  toner particles is capable of producing  $84.67 \mu\text{m}$  'dots' or features, sub-resolvable in terms of the wavelength of the interrogating ultrasound beam (Schein 1992).

## 2.4. Randomized patterns

Unstructured or randomized scatterer patterns are preferred for evaluation of broadband spatial frequency response. This is because regular, periodic scattering profiles will produce frequency-dependent changes in an ultrasound speckle pattern (Tuthill *et al* 1988). An example of unstructured patterns of digital scatterers and the resultant ultrasound image of a test object produced with these patterns is illustrated in figure 2. The scattering areas are generated by the 'Blue Noise Mask' (BNM), a digital halftone screen that produces unstructured patterns with carefully controlled power spectra (Yao and Parker 1994, Mitsa and Parker 1992). It is important to recognize that there is not a simple

one-to-one correspondence between the speckle pattern shown in the ultrasound image and the individual ‘dots’ in the BNM patterns. Rather, the speckle results from the complex interaction of the scattering waves produced by each deposited scatterer. A greater number of ‘minority’ scattering sites per unit area will produce a greater echogenicity. An alternative to varying scattering number per unit area would be to vary either the thickness, density or speed of sound of the deposited scattering material in relation to its position. For example, a process similar to ‘multi-toning’ can be used to incorporate multiple levels of scattering sites on a substrate. Alternatively, different scattering strengths could be achieved via sets of different scatterer types, each possessing different scattering strengths. In most situations, simple modulation of the concentration of uniform scatterers is sufficient to provide the desired variations in echogenicity.

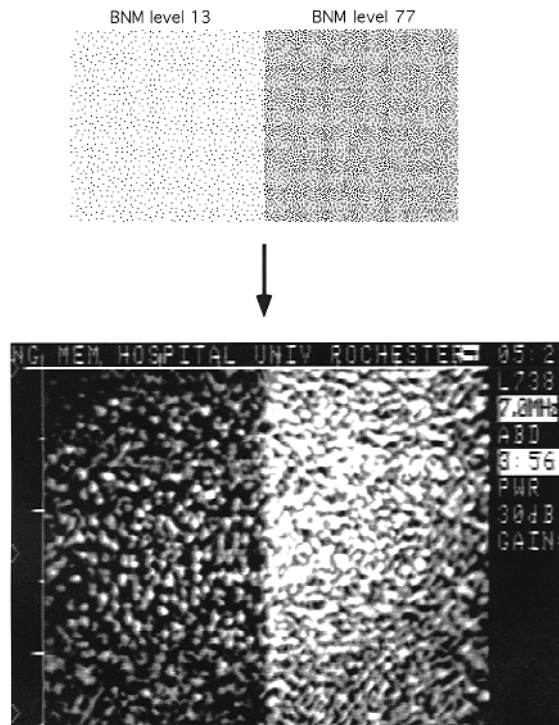


**Figure 2.** Examples of Blue Noise Mask (BNM) half-tone patterns and resultant ultrasound images at 7 MHz.

### 2.5. Thin film test object manufacturing requirements

It is preferable to incorporate a thin, stable, nominally rigid substrate with an acoustic impedance relatively similar to physiological saline ( $Z_{\text{saline}} = 1.54 \times 10^6 \text{ Pa s m}^{-1}$ ). Fortunately, the effect of the substrate on the local acoustic impedance and speed of sound becomes very weak in the limit as the substrate thickness becomes small compared with the wavelength of the imaging pulse. As mentioned above, the scattering material must have an acoustic impedance relatively dissimilar from physiological saline while at the same time exhibiting good stability when immersed in a saline solution (or other appropriate

propagating medium) and have the capacity to be deposited in a uniform film, in terms of both material properties and thickness.

A substrate such as glass or even quartz might lend itself to these techniques, and would certainly remain stable when immersed in an aqueous solution. However, both substances have a significantly different acoustic impedance with respect to water ( $Z_{\text{water}} = 1.48 \times 10^6 \text{ Pa s m}^{-1}$ ,  $Z_{\text{glass (Pyrex, bar)}} = 12.0 \times 10^6 \text{ Pa s m}^{-1}$ ,  $Z_{\text{quartz (X-cut, bar)}} = 14.5 \times 10^6 \text{ Pa s m}^{-1}$  (Kinsler *et al* 1982)). A nylon, polystyrene or Lucite substrate with an acoustic impedance more closely matched to water ( $Z_{\text{nylon (6-6, bar)}} = 2.00 \times 10^6 \text{ Pa s m}^{-1}$ ,  $Z_{\text{polystyrene (bar)}} = 2.37 \times 10^6 \text{ Pa s m}^{-1}$ ,  $Z_{\text{Lucite (bar)}} = 2.15 \times 10^6 \text{ Pa s m}^{-1}$  (Kinsler *et al* 1982, Weast 1969)) lends itself more favourably to less expensive procedures such as lithography and electrostatic printing.

### 3. Methods

Due to readily available, low cost and well developed computer interfaces for pattern transfer via laser printing, initial test objects were generated using 300 and 600 dpi laser printers. Some of the patterns were first printed on common 20 lb copier paper and then transferred to Kodak Ektaprint Transparency Material (Cat 151 4793) using a Kodak Ektaprint Model 225 copier-duplicator system (Kodak, Rochester, NY). Some of the patterns were printed directly on to the transparency material with a DEClaser 1152 300 dpi laser printer (Digital Equipment Corporation, Boston, MA).

Pieces of transparency material approximately  $7.6 \text{ cm} \times 12.7 \text{ cm}$  with patterns ranging from  $3.8 \text{ cm}^2$  to  $6.4 \text{ cm} \times 7.6 \text{ cm}$  in size were placed in a u-shaped acrylic frame that provided rigid support of the test object as it was imaged. The blank copier transparency material had a nominally measured thickness of  $132 \mu\text{m}$  and that of the transparency with pattern  $142 \mu\text{m}$ , providing a  $10 \mu\text{m}$  pattern thickness. The edges of the transparency parallel to the face of the transducer were abraded with emery cloth or cut at random angles in an effort to minimize specular reflections and possible reverberation artifacts from those surfaces.

The transparency and the acrylic frame were placed in a  $17.8 \times 12.7 \times 30.5 \text{ cm}$  (H $\times$ W $\times$ L, inner dimensions) Plexiglass tank filled with degassed tap water at room temperature. The frame was arranged so that the transparency would lie in the scanning plane of the imaging transducer. Either a Quantum QAD-1 (Quantum, Issaquah, WA presently Siemens, Seattle, WA) scanning system with a 5 or 7.5 MHz linear array transducer or an Acuson 128/XP10 (Acuson, Mt View, CA) imaging system with a 5 or 7 MHz linear array transducer was used to image the test object. The transducer was placed in direct contact with the water surface and held in alignment with the test object by a common laboratory ring-stand and test-tube clamp. In an attempt to avoid initial ring down artifacts and edge effects from the transparency material, the pattern was positioned more than 1 cm below the proximal edge of the transparency material which was then placed adjacent to the transducer face (figure 3). Once a suitable image was obtained (using a flat time/gain compensation), it was either captured and stored in TIFF file format on a 386DX based PC compatible computer equipped with an Imaging Technology PCVisionplus (Imaging Technology, Woburn, MA) video acquisition board and the JAVA video analysis software package (Jandel Scientific, Corte Madera, CA) utilizing the video output from the QAD-1 rear panel or, in the case of the Acuson 128/XP10, recorded to VHS or SVHS videotape and then captured by the same computer system in an off-line manner.

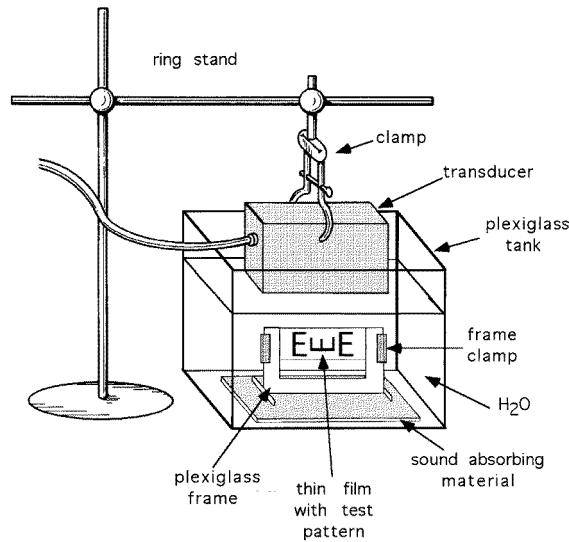


Figure 3. Experimental configuration.

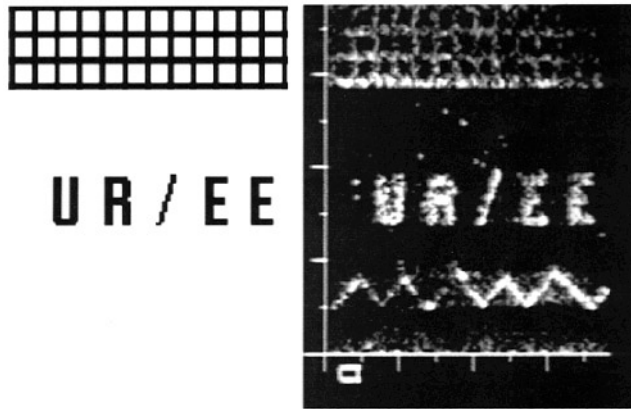
#### 4. Results

To facilitate initial evaluation, relatively straightforward patterns consisting of lines, dots and upper case alphanumeric characters were used (figures 4(a) and 4(b)). A more complex circular grid exhibits a degradation of resolution in the diverging field beyond the focal zone (figure 4(c)). A gray scale pattern was imaged as a test of half-tone techniques (figure 2).

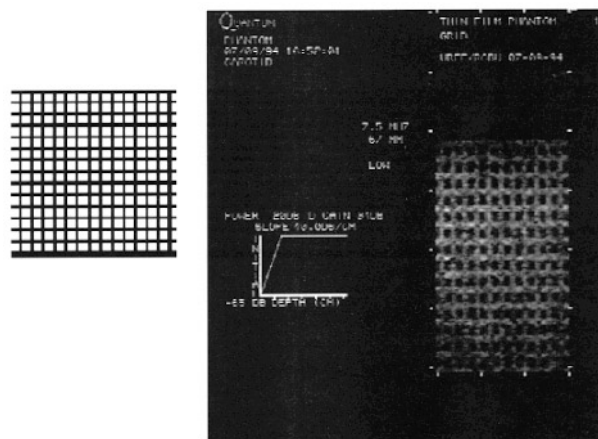
Figure 2 consists of a pattern generated utilizing the Blue Noise Mask. The level corresponds to the number of printed or dark dots in a given area of interest out of a maximum of 256. The test pattern was produced on a 300 dpi printer with each printed dot having a height and width of approximately  $85 \mu\text{m}$ . The grids shown in figures 4(a) and 4(b) consist of 0.8 mm thick lines with a spacing of 2.4 mm. Since the targets were immersed in water, in which sound has a lower speed than in tissue ( $1490 \text{ m s}^{-1}$  versus  $1540 \text{ m s}^{-1}$ ), the vertical aspect of the image appears slightly elongated. This is also evident in figure 4(c), which is an image of a circular grid pattern of 0.3 mm thick lines. The grid has an overall diameter of 51 mm and inner circles with radii measuring 6.35 mm, 12.7 mm and 19.05 mm.

Figures 2, 4(a) and 4(c) were obtained with the Acuson 128/XP10 utilizing an L738 7 MHz linear array transducer. Figure 4(b) was obtained with the Quantum QAD-1 using a 7.5 MHz linear array transducer.

The ability to make precise line targets makes it possible to assess direction-related resolution and spatial frequency response by inspection, thus facilitating the implementation of a simple evaluation procedure. Simplified vertical and horizontal 'chirp' patterns were generated with alternating pairs of equal width lines and spaces that ranged in width (or spatial frequency) as shown in figure 5(a). The pattern was immersed in degassed water at room temperature and scanned with the Quantum QAD-1 using 5 MHz and 7.5 MHz linear array transducers. Care was taken to ensure that the power and gain settings were equivalent and the displayed brightness within the pattern was not saturated (slope:  $0 \text{ dB cm}^{-1}$ , 5 and 7.5 MHz; power:  $-10 \text{ dB}$ , 5 and 7.5 MHz; initial:  $-10 \text{ dB}$ , 5 MHz,  $-9 \text{ dB}$ ,



(a)

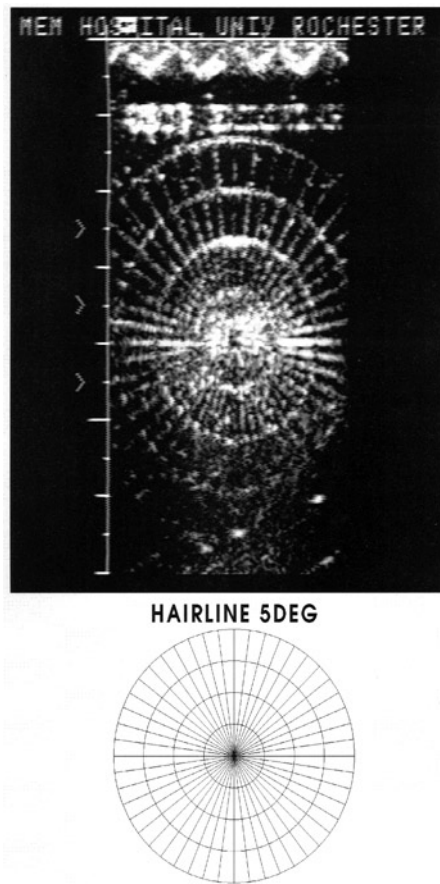


(b)

**Figure 4.** (a) Example of Acuson 128XP scan, 7 MHz transducer; the original pattern used to produce thin film is on the left. (b) Example of Quantum QAD-1 scan, 7.5 MHz transducer; original pattern on the left. (c) Example of Acuson 128XP scan, 7 MHz transducer; the original pattern used to produce the thin film is below.

7.5 MHz; displayed brightness assessed using green tag function in continuous mode). The images were digitally captured and redisplayed on a high-quality JVC TM-1400SU (Victor Company of Japan, Yokohama, Japan) video monitor to facilitate scoring. Five observers visually compared the displayed images and were asked to count the number of lines they could resolve in the four quadrants of the pattern up to the smallest line they could resolve. Accuracy and reproducibility is limited by the quantization of the line widths and intraobserver variability. In the experiment, line widths ranged from 0.2 mm to 1.8 mm (2.5 lines/mm to 0.28 lines/mm). Figure 5 shows the line pair test pattern and the images produced from the scans at 5 MHz and 7.5 MHz. Table 1 shows the results of the five test subjects who evaluated the images.

As would be expected, resolution of the horizontal lines by the 7.5 MHz transducer was superior to the 5 MHz transducer. Resolution of the vertical lines was approximately the same, although there was a higher variation of the observations obtained from the 7.5 MHz



(c)

**Figure 4.** (Continued)

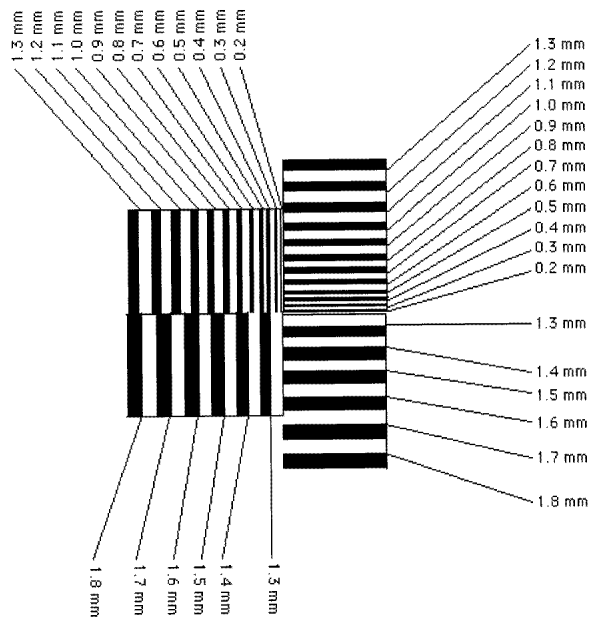
image. The manufacturer's specifications for the  $-6.0$  dB image resolutions in tissue were 0.26 mm (axial) and 0.8 mm (lateral) for the 7.5 MHz transducer and 0.38 mm (axial) and 1.4 mm (lateral) for the 5 MHz transducer.

## 5. Discussion

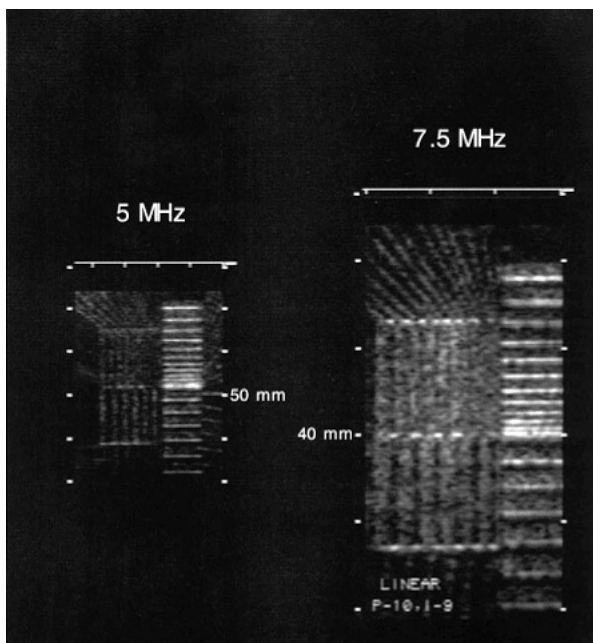
The thin film test object incorporating digital scatterers makes possible new and useful imaging test patterns. As such, it may find utility in endeavours ranging from basic system performance investigation to routine quality assurance tasks. In fact, the thin film test object under consideration could be implemented in a number of ways for general-purpose quality-assurance use. For the sake of conciseness, we will focus on its simplest implementation.

A basic configuration consists of a thin film object with a pattern (or patterns) fixed in any number of the currently available tissue mimicking phantom media and can even be included in any one of the current solid target type (wires, inclusions, etc) phantoms. It is also possible to include multiple, parallel thin film test objects in a single phantom. Other implementations, similar to that used for experimental measurements, can incorporate





(a)



(b)

**Figure 5.** (a) Resolution experiment target pattern. Line widths are as indicated. (b) Resolution experiment images. Images acquired with an Quantum QAD-1 scanner utilizing linear array transducers operating at 5 MHz (left) and 7.5 MHz (right). Images are displayed in same proportion as on the scanner display. Horizontal and vertical distance markers represent 10 mm increments. 5 MHz settings: slope  $0 \text{ dB cm}^{-1}$ , power  $-10 \text{ dB}$ , initial  $-10 \text{ dB}$ . 7.5 MHz settings: slope  $0 \text{ dB cm}^{-1}$ , power  $-10 \text{ dB}$ , initial  $-9 \text{ dB}$ .

**Table 1.** Results of the line pair resolution experiment based on observations of five subjects. Horizontal refers to horizontal (aligned with azimuthal axis) lines, vertical refers to vertical (aligned with depth axis) lines. Mean widths for the smallest line resolved are rounded to the nearest 0.1 mm and mean spatial frequencies are rounded to the nearest 0.1 line pair (lp) per millimetre. SD: standard deviation.

Transducer	Smallest resolvable line width			
	Mean width (mm)		SD (mm)	
	Horizontal	Vertical	Horizontal	Vertical
5 MHz	0.4	1	$4.5 \times 10^{-2}$	$5.5 \times 10^{-2}$
7.5 MHz	0.2	1	$4.5 \times 10^{-2}$	$2.7 \times 10^{-1}$

Transducer	Highest resolvable spatial frequency			
	Mean (lp mm <sup>-1</sup> )		SD (lp mm <sup>-1</sup> )	
	Horizontal	Vertical	Horizontal	Vertical
5 MHz	1.3	0.5	$1.9 \times 10^{-1}$	$3.0 \times 10^{-2}$
7.5 MHz	2.3	0.5	$3.7 \times 10^{-1}$	$1.8 \times 10^{-1}$

changeable thin film targets immersed in suitable test fluid. These embodiments include a guide (or guides) for alignment purposes and possibly ruled demarcations of lengths and/or angles for analysis purposes (e.g. to measure beam thickness or actual angle of the scan plane from a plane perpendicular to the face of the transducer). Although initial evaluations have been performed in non-scattering and relatively unattenuating propagating fluids, current work involves embedding of the target in a variety of scattering and attenuating gels and fluids such as 1,3 butanediol, which exhibits frequency-dependent attenuation characteristics.

Overall, this type of phantom should enable a direct method for quantifiable, repeatable and reliable assessment of performance across all levels of an ultrasound scanner's imaging chain. In terms of the actual imaging equipment, it will allow detection and quantification of factors such as resolution in line pairs per millimetre or the system modulation transfer function. As evidenced from the results of the line width target and image depicted in figures 5(a) and 5(b), even simple patterns can be used to illuminate subtle system response characteristics.

From a broader perspective, given some of the currently available electrophotographic/copier/laser printer technologies that incorporate a variety of conductive and magnetic toner particles (Dessauer and Clark 1965, Schein 1992), this type of thin film test object may find applicability for producing phantoms used in quality assurance procedures for other areas of radiological imaging such as MRI and CT by taking advantage of some of the radio-opaque compounds which contain iron, lead, iodine and other higher-energy absorbing elements as well as paramagnetic materials.

## 6. Conclusion

This paper describes a novel approach for constructing an ultrasound imaging test object using thin films and precise positioning of 'digital' scattering patterns. This approach permits assessment of ultrasonic scanning system characteristics in terms of established imaging science standards. It provides sophisticated test patterns which can be used to augment the performance evaluations which are currently available for diagnostic ultrasound scanners.

The variety of complex patterns it affords can enable multiple image analysis measurements to be performed from the scan of a single test object. Further, these test objects may be easily incorporated into currently used ultrasound imaging phantoms to add to their recognized test capabilities and overall utility.

## References

- AIUM 1991 *Standard Methods for Measuring Performance of Pulse-Echo Ultrasound Imaging Equipment* (Rockville, MD: American Institute of Ultrasound in Medicine)
- Alasaarela E and Koivukangas J 1990 Evaluation of image quality of ultrasound scanners in medical diagnosis *J. Ultrasound Med.* **9** 23–34
- Archer-Hall J A and Hutchins D A 1979 The photoelastic visualization of ultrasonic waves in liquid *Ultrasonics* September 209–12
- 1981 The effectiveness of thin layers as ultrasonic visualization media *Ultrasonics* March 77–80
- ATS Laboratories Inc 1993 *Product Literature* (Bridgeport, CT: ATS Laboratories)
- Carlson F P 1977 *Introduction to Applied Optics for Engineers* (New York: Academic)
- Cone Instruments 1993 *Ultrasound Supplies and Accessories* vol 15 (Solon, OH: Cone Instruments)
- Dainty J C and Shaw R 1974 *Image Science: Principles, Analysis and Evaluation of Photographic-type Imaging Processes* (New York: Academic)
- Dessauer J H and Clark H E 1965 *Xerography and Related Processes* (New York: Focal Press)
- Goldstein A and Clayman W 1983 Particle image-resolution test object *J. Ultrasound Med.* **2** 195–209
- Hill C R, Bamber J C, Crawford D C, Lowe H J and Webb S 1991 What might echography learn from image science? *Ultrasound Med. Biol.* **17** 559–75
- Hill C R and Kratochwil A 1981 *Medical Ultrasonic Images: Formulation, Display, Recording and Perception* (Amsterdam: Excerpta Medica)
- Kinsler L E, Frey A R, Coppers A B and Sanders J V 1982 *Fundamentals of Acoustics* (New York: Wiley)
- Madsen E L, Zagzebski J A, Banjavie R A and Jutila R E 1978 Tissue mimicking materials for ultrasound phantoms *Med. Phys.* **5** 391–4
- Madsen E L, Zagzebski J A and Ghilardi-Netto T 1980 An anthropomorphic torso section phantom for ultrasonic imaging *Med. Phys.* **7** 43–50
- Mitsa T and Parker K J 1992 Digital halftoning technique using a blue-noise mask *J. Opt. Soc. Am. A* **9** 1920–9
- Morse P M and Uno K U 1986 *Theoretical Acoustics* (Princeton, NJ: Princeton University Press)
- Ophir J, Maklad N and Jeger P 1983 Ultrasonic beam characterization device *United States Patent* 4,406,153 (Washington, DC: United States Patent Office)
- Rose A and Weimer P K 1989 Physical limits to the performance of imaging systems *Phys. Today* September 24–32
- Schein L B 1992 *Electrophotography and Development Physics* (Berlin: Springer)
- Smith S W 1982 A contrast-detail analysis of diagnostic ultrasound imaging *Med. Phys.* **9** 4–12
- Sommer F G, Filly R A, Edmonds P D, Reyes Z and Comas M E 1980 Technical note: a phantom for imaging biological fluids by ultrasound and CT scanning *Ultrasound Med. Biol.* **6** 135–40
- Spitzer V M, Carson P L, Scherzinger A L and Carter W 1979 Evaluation of ultrasonic array image quality *Med. Phys.* **6** 350
- Tuthill T A, Sperry R H and Parker K J 1988 Deviations from Rayleigh statistics in ultrasonic speckle *Ultrasonic Imaging* **10** 81–9
- Weast R C 1969 *CRC Handbook of Chemistry and Physics* College edn (Cleveland, OH: The Chemical Rubber Company)
- Yao M and Parker K J 1994 Modified approach to the construction of a blue noise mask *J. Electron. Imaging* **3** 92–7
- Yao L X, Zagzebski J A and Madsen E L 1991 Statistical uncertainty in ultrasonic backscatter and attenuation coefficients determined with a reference phantom *Ultrasound Med. Biol.* **17** 187–94